ISSN 1392–1207. MECHANIKA. 2015 Volume 21(2): 91–98

Description of stress fields and displacements at the tip of a rigid, flat inclusion located at interface using modified stress intensity factors

G. Mieczkowski
Białystok University of Technology, ul. Wiejska 45C, 15-351 Białystok, Poland, E-mail: g.mieczkowski@pb.edu.pl

crossref http://dx.doi.org/10.5755/j01.mech.21.2.8726

1. Introduction

Development of technologies for the production of composite structures, allowing forming materials with specific strength and performance properties has resulted in their frequent use in machinery and construction engineering. The homogenous components selected in suitable proportions, when combined together, provide greater rigidity and strength, while reducing the weight.

The composite materials are characterized by macroscopic inhomogeneity of their structures. Forced compliance of surface displacements in relation to combination of components with different rigidity and potential presence of discontinuities in materials or sharp inclusions which cause local high stress gradients might be observed here. Such concentrators can generate a singular stress field of qualitatively different nature than in the case of stress raisers arranged in a homogeneous material. In many theoretical works on sharp corners with different boundary conditions [1-5] it has been proved that the exponent λ can take different real or complex values.

Mechanical description of the stress fields in flat rigid inclusion area was dealt with by many scientists [6-11]. Wang et al. [6] have shown that for inclusions located on a homogeneous material the stress fields were described by identical exponent as in case of the crack. Ballarini [7] proposed, in form of integral equations, equations describing the stress field and a strict solution of the stress intensity factors. Wu [8] and Ballarini [9] extended it to an issue of inclusions located at the interface. Ballarini suggested functions of complex potentials [12] to be used for analysis of the issues. Assuming that a flat, rectangular disk is impacted infinitely by tensile loads he has received, in a complex form, dependences describing components of stress at the sharp tip of the inclusion. Furthermore, he gave a solution close to the stress intensity factors used in description of the tested fields.

The analytical dependences for calculating coefficients K_I and K_{II} [9] can only be used assuming that on the plate there is an infinitely applied operating longitudinal and transverse tensile load. In case of finite dimensions of the component or the presence of additional inclusions or cracks when introducing abnormal stress distribution, it is necessary to use methods of determining numerical values for the sought coefficients.

This was set in the work by Dong [13], Mochalov and Sil'vestrov [14] for different configurations of inclusions and cracks using the appropriate integral equations. Basing on comparison of stresses obtained using the BEM with the analytical solution, Lee and Kwak [15] have defined the stress intensity factors of the first particular member.

2. Main purposes of the work

In this case, alike the issue of interfacial crack, the exponent is a complex number. Thus, the stress fields have an oscillating feature [2], which hinders their analytical description. The use of fracture mechanics hypotheses based on local stress fields (eg Sih, McClintock) requires oscillations to be eliminated from the analytical description. Therefore the main purpose of this work is to obtain an analytical description of the mechanical fields without applying oscillation. In order to get such description the classic definition of stress intensity factors K_I and K_{II} with appropriately modified counterparts $K_I^{\lambda_r}$ and $K_{II}^{\lambda_r}$ needs to be replaced taking into account oscillating nature of the singular stress field. In the literature there can rarely be found an analytical description of fields of stresses and displacements in the area of sharp inclusions at the interface with use of the so-modified actual coefficients $K_I^{\lambda_r}$ and $K_{II}^{\lambda_r}$. It was necessary to find relationship between the classically defined stress intensity factors K_I and K_{II}, as well as an adopted analytical description of the modified $K_I^{\lambda_r}$ and $K_{II}^{\lambda_r}$. Another purpose of the study was to develop a method on how to calculate the modified stress intensity factors $K_j^{\lambda_r}$. In this case, in order to determine the value of modified coefficients $K_I^{\lambda_r}$ and $K_{II}^{\lambda_r}$ and also higher order terms coefficients of the asymptotic solutions, the FEM has been applied, what found its positive verification for issues related to the interfacial crack [16].

3. The method and the results of analytical calculations

The approach proposed in the work by Parton and Perlin [17] served basis for obtaining, as an asymptotic, analytical description of the fields of stresses and displacements at the tip of a sharp rigid inclusion (using modified stress intensity factor) (Fig. 1).

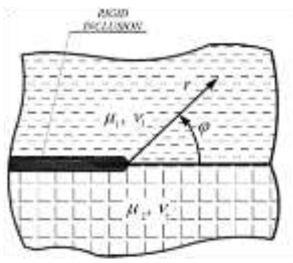

Fig. 1 Sharp, rigid inclusion located on border of merger of two elastic materials

Parton and Perlin took into consideration a flat, sharp corner of side angle 2β, found as a result in a linear-elastic material, the polar coordinate system (r, φ) positioned at the tip (Fig. 2).The authors have received a general solution of the sharp corner problem in the form of components of displacement and stress fields:

$$\left.\begin{aligned}
u_r &= r^{\lambda}\left(A\cos\left((1+\lambda)\varphi\right)+B\sin\left((1+\lambda)\varphi\right)+C\cos\left((1-\lambda)\varphi\right)+D\sin\left((1-\lambda)\varphi\right)\right),\\
u_\varphi &= r^{\lambda}\left(-A\sin\left((1+\lambda)\varphi\right)+B\cos\left((1+\lambda)\varphi\right)-C\frac{\kappa+\lambda}{\kappa-\lambda}\sin\left((1-\lambda)\varphi\right)+D\frac{\kappa+\lambda}{\kappa-\lambda}\cos\left((1-\lambda)\varphi\right)\right),\\
\sigma_r &= r^{\lambda-1}\mu\left(A2\lambda\cos\left((1+\lambda)\varphi\right)+B2\lambda\sin\left((1+\lambda)\varphi\right)+C(3-\lambda)\frac{2\lambda}{\kappa-\lambda}\cos\left((1-\lambda)\varphi\right)+D(3-\lambda)\frac{2\lambda}{\kappa-\lambda}\sin\left((1-\lambda)\varphi\right)\right),\\
\sigma_\varphi &= r^{\lambda-1}\mu\left(-A2\lambda\cos\left((1+\lambda)\varphi\right)-B2\lambda\sin\left((1+\lambda)\varphi\right)+C(1+\lambda)\frac{2\lambda}{\kappa-\lambda}\cos\left((1-\lambda)\varphi\right)+D(1+\lambda)\frac{2\lambda}{\kappa-\lambda}\sin\left((1-\lambda)\varphi\right)\right),\\
\tau_{r\varphi} &= r^{\lambda-1}\mu\left(-A2\lambda\sin\left((1+\lambda)\varphi\right)+B2\lambda\cos\left((1+\lambda)\varphi\right)+C(1-\lambda)\frac{2\lambda}{\kappa-\lambda}\sin\left((1-\lambda)\varphi\right)-D(1-\lambda)\frac{2\lambda}{\kappa-\lambda}\cos\left((1-\lambda)\varphi\right)\right).
\end{aligned}\right\}\quad(1)$$

Four independent constants A, B, C, D can be determined from the boundary conditions of concerned problems, while the value of the exponent λ is determined by *characteristic equation* representing the determinant zero boundary conditions.

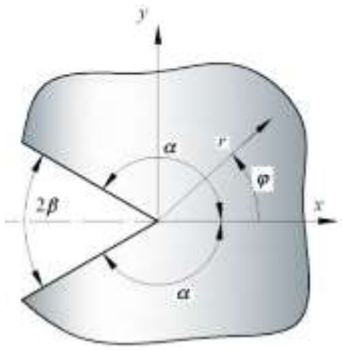

Fig. 2 Location of the tip of a sharp notch in linear-elastic material

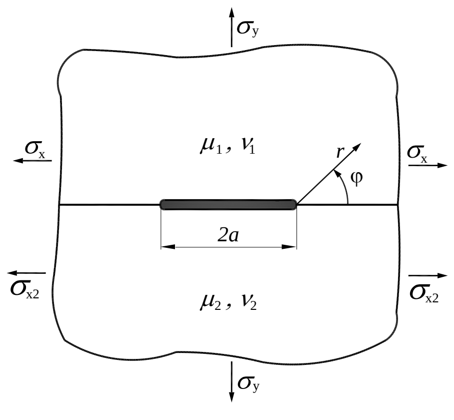

Fig. 3 Sharp, rigid inclusion located on the interface

When considering this work an issue of sharp, rigid inclusions, situated between two elastic materials (Fig. 3), was taken into account until meeting the following eight boundary conditions:

1- of upper surface of rigid inclusions, for $\varphi = \pi$:

$$u_{\varphi 1} = 0; u_{r1} = 0\,;$$

2- of lower surface of rigid inclusions, for $\varphi = -\pi$:

$$u_{\varphi 2} = 0; u_{r2} = 0\,;$$

3- along the interface, for $\varphi = 0$:

$$u_{r1} = u_{r2}; u_{\varphi 1} = u_{\varphi 2};\ \sigma_{\varphi 1} = \sigma_{\varphi 2}; \tau_{r\varphi 1} = \tau_{r\varphi 2}\,.$$

Characteristic equation results from the following formula:

$$\lambda\sin[\pi\lambda]\left(\begin{gathered}\Gamma^2\kappa_2^2+\kappa_1^2\left(\begin{gathered}1+2\left(\Gamma+\cos[2\pi\lambda]\right)\kappa_2+\\ \left(1+\Gamma^2+2\Gamma\cos[2\pi\lambda]\right)\kappa_2^2\end{gathered}\right)+\\ +2\Gamma\kappa_1\kappa_2\left(\kappa_2+\cos[2\pi\lambda](1+\Gamma\kappa_2)\right)\end{gathered}\right)=0, \quad (2)$$

where Γ is denotes the ratio of shear modulus μ_1/μ_2, while $\kappa_j = 3 - 4v_j$ - a plane strain. In consequence, the result of Eq. (2) represents λ exponent value.

The result shows that there is one singular term of asymptotic solution for complex exponent, the real part λ_r of which is always 0.5, and imaginary part ε depends on the structure of material constants and can be determined on basis of the below equation:

$$\epsilon = \frac{1}{2\pi}\log\left[\frac{\kappa_2\left(\mu_1+\kappa_1\mu_2\right)}{\kappa_1\left(\kappa_2\mu_1+\mu_2\right)}\right]. \quad (3)$$

Subsequent units are suitable: 1, 1.5 + ϵ, 2, 2.5 + ϵ.

Analytical formulas describing components of the stress field and displacements around the tip of inclusion Eq. (4) have also been obtained:

$$\left.\begin{aligned}
\sigma_{ik} &= \frac{\mathrm{e}^{-\epsilon\varphi}\left(K_I^{\lambda_r}f_{ik}^{I}+K_{II}^{\lambda_r}f_{ik}^{II}\right)}{2\sqrt{2\pi r}\left(1+\kappa_j\right)\left(-1+\mathrm{e}^{2\pi\epsilon}\kappa_j\right)},\\
u_i &= \frac{\sqrt{r}\mathrm{e}^{-\epsilon\varphi}\left(K_I^{\lambda_r}g_i^{I}+K_{II}^{\lambda_r}g_i^{II}\right)}{2\sqrt{2\pi}\left(1+4\epsilon^2\right)\left(1+\kappa_j\right)\left(-1+\mathrm{e}^{2\pi\epsilon}\kappa_j\right)\mu_j}.
\end{aligned}\right\}\quad(4)$$

The modified stress intensity factors are defined as follows:

$$\left.\begin{aligned}
K_I^{\lambda_r} &= \lim_{r\to 0}\sqrt{2\pi r}\begin{pmatrix}\cos\left[\epsilon\log[r]\right]\sigma_\varphi(r,0)-\\ \sin\left[\epsilon\log[r]\right]\tau_{r\varphi}(r,0)\end{pmatrix},\\
K_{II}^{\lambda_r} &= \lim_{r\to 0}\sqrt{2\pi r}\begin{pmatrix}\sin\left[\epsilon\log[r]\right]\sigma_\varphi(r,0)+\\ \cos\left[\epsilon\log[r]\right]\tau_{r\varphi}(r,0)\end{pmatrix}.
\end{aligned}\right\}\quad(5)$$

Functions (materials constants and in polar coordinates reference) f_{ik}^{I}, f_{ik}^{II} and g_i^{I}, g_i^{II} are given in the Appendix.

Relations between the classically defined stress intensity factors K_I and K_{II} and an adopted analytical description of the modified factors $K_I^{\lambda_r}$ and $K_{II}^{\lambda_r}$ can be written as follows:

$$\left.\begin{aligned} K_I^{\lambda_r} &= K_I\, cos\left[\epsilon\, log\left[2a\right]\right] - K_{II}\, sin\left[\epsilon\, log\left[2a\right]\right], \\ K_{II}^{\lambda_r} &= K_{II}\, cos\left[\epsilon\, log\left[2a\right]\right] + K_I\, sin\left[\epsilon\, log\left[2a\right]\right]. \end{aligned}\right\} \tag{6}$$

For sharp inclusions at the interface, classically defined factors K_I and K_{II} [9] can be calculated from the following equation:

$$\left.\begin{aligned} K_I &= \frac{-\sqrt{\pi a}\left(cos\left[\epsilon Log\left[2a\right]\right] + 2\epsilon\, sin\left[\epsilon Log\left[2a\right]\right]\right)\left(-1+\kappa_1\kappa_2\right)\mu_2\left(\left(1+\kappa_1\right)\sigma_x + \left(-3+\kappa_1\right)\sigma_y\right)}{4\left(1+\kappa_1\right)\kappa_2\mu_1 + 4\kappa_1\left(1+\kappa_2\right)\mu_2}, \\ K_{II} &= \frac{-\sqrt{\pi a}\left(2\epsilon\, cos\left[\epsilon Log\left[2a\right]\right] - sin\left[\epsilon Log\left[2a\right]\right]\right)\left(-1+\kappa_1\kappa_2\right)\mu_2\left(\left(1+\kappa_1\right)\sigma_x + \left(-3+\kappa_1\right)\sigma_y\right)}{4\left(1+\kappa_1\right)\kappa_2\mu_1 + 4\kappa_1\left(1+\kappa_2\right)\mu_2}, \end{aligned}\right\} \tag{7}$$

where a is half the length of inclusions, σ_y and σ_x are applied tensile load in the infinity (longitudinal - σ_x and transverse - σ_y).

4. FEM application results

Using the FEM (ANSYS), a bimaterial structure was modeled with rigid inclusion in the interface line (Fig. 4, a). Length of $2a$ inclusions is small in relation to the height h and the width b of the disc (a = 1, b = h = = 20a), which corresponds to the issue of inclusions in the "infinite" area. Shield described quadrangular, finite elements with increased density found in the tip area (Fig. 4, b), with special triangular elements surrounding singular point [18].

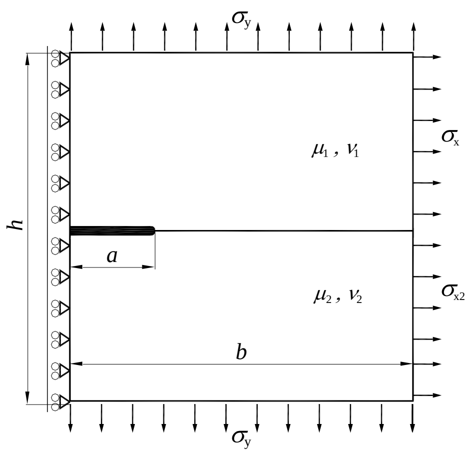

a

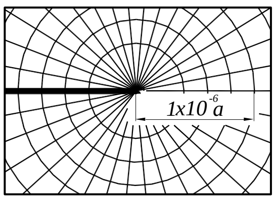

b

Fig. 4 a – FEM modeled fragment of structure, where a = 1, b = h = 20, b - of finite elements around tip of inclusion

This inclusion has been modeled using a special rigid beam of finite elements (ANSYS, element type: MPC184). Because of symmetry, only half of the disc was modeled. In order to ensure equality displacements at right side of the disc, load value σ_{x2} [19] is dependent on components σ_x and σ_y:

$$\sigma_{x2} = \frac{4\beta - 2\alpha}{1-\alpha}\sigma_y + \frac{1+\alpha}{1-\alpha}\sigma_x\,, \tag{8}$$

where

$\alpha = \dfrac{\mu_2\left(\kappa_1+1\right) - \mu_1\left(\kappa_2+1\right)}{\mu_2\left(\kappa_1+1\right) + \mu_1\left(\kappa_2+1\right)}, \beta = \dfrac{\mu_2\left(\kappa_1-1\right) - \mu_1\left(\kappa_2-1\right)}{\mu_2\left(\kappa_1+1\right) + \mu_1\left(\kappa_2+1\right)}$ is Dundurs' [19] constants.

Numerical calculations were designed to determine the value of modified coefficients $K_I^{\lambda_r}$, $K_{II}^{\lambda_r}$, to compare theses to the exact solution (7), using Eq. (6).

Typically, in order to determine the stress intensity factors (using the FEM) the following four methods are used:

1. comparison of stresses or displacements resulting from the FEM solution with a known analytical solution [20];
2. determination of the value of integral J on basis of the FEM [21];
3. designation of sought coefficients on basis of the change in strain energy associated with growth of virtual cracks [22];
4. use of special finite elements [23].

For aspects concerning this work not all the above methods can be used (e.g., 3), and some have certain limitations. At the same time, in case of the analytical solution components of stress always depend on factors $K_I^{\lambda_r}$ and $K_{II}^{\lambda_r}$, thus when using method 2, there can only be determined the value of integral J, which is functionally related to the sum of the squares of the sought coefficients. Therefore it is impossible to calculate $K_I^{\lambda_r}$ and $K_{II}^{\lambda_r}$ values separately. When using the FEM modeling commercial software, it is not always simple to apply their own finite elements, allowing direct determination of sought coefficients.

Knowing the analytical solution of stress distribution and displacements, it seems reasonable to use method 1 to determine coefficients $K_I^{\lambda_r}$ and $K_{II}^{\lambda_r}$ for work issues analyzed in case of sharp inclusions. It is settled in approximation. Values of the stress / displacement obtained from the FEM solutions have approximated special functions correlated to the analytical solution. In case of displacements of the fields, the FEM and analytical solutions were compared for two angles φ = 0 and $\pi/2$, and the stress distribution for three φ = 0, $\pi/2$ and π. The best results (presented hitherto in the work) based on the stress fields for angle φ = 0 (φ - polar angle in polar coordinates – Fig. 1) have been obtained.

Disadvantage of this method, however, is the need for providing high density mesh division into finite elements around the tip of stress concentrator. Additionally, accuracy of the results is affected by the selection area where the numerical solution is compared to the analytical one. The drawback of this can eliminate by the use of higher order terms $K_{ji}^{\lambda_r}$ in asymptotic expansion [24, 25]. For the issues analyzed three elements have been included. Approximating functions used herein are as follows:

$$\left.\begin{aligned} F_{\mathrm{I}} &= \sqrt{2\pi r}\left(cos\left[\epsilon\, log\left[r\right]\right]\sigma_{\varphi}\left(r,0\right) - sin\left[\epsilon\, log\left[r\right]\right]\tau_{r\varphi}\left(r,0\right)\right) = K_{I}^{\lambda_r} + K_{I2}^{\lambda_r}\sqrt{r} + K_{I3}^{\lambda_r} r + \ldots, \\ F_{\mathrm{II}} &= \sqrt{2\pi r}\left(sin\left[\epsilon\, log\left[r\right]\right]\sigma_{\varphi}\left(r,0\right) + cos\left[\epsilon\, log\left[r\right]\right]\tau_{r\varphi}\left(r,0\right)\right) = K_{II}^{\lambda_r} + K_{II2}^{\lambda_r}\sqrt{r} + K_{II3}^{\lambda_r} r + \ldots. \end{aligned}\right\}$$

Values of modified stress intensity factors $K_j^{\lambda_r}$ and coefficients of higher order terms $K_{ji}^{\lambda_r}$ for different variants of the load are provided in Tables 1 and 2 and in Figs. 5-8. In order to investigate the sensitivity of the method chosen for variation of material constants, calculations were performed for two-phase structures with different proportions of the Young's modules Γ_0 and Poisson's ratios ν_0. The study was based on: E_1 = 10000000, ν_1 = 0.25.

Table 1

Values of coefficients $K_j^{\lambda_r}\ /\ a$ for tensile perpendicular to interface

$\nu_0 = \nu_2 / \nu_1$	$\Gamma_0 = E_2 / E_1$	$K_I^{\lambda_r} / a$	$K_I^{\lambda_r *} / a$	*Error*, %	$K_{II}^{\lambda_r} / a$	$K_{II}^{\lambda_r *} / a$	*Error*, %
0	10	25.08	25.41	1.30	7.29	7.46	2.34
0.5	10	22.80	23.09	1.29	5.56	5.57	0.07
1	10	19.84	20.14	1.50	3.49	3.59	2.81
0	5	23.64	23.47	0.74	5.71	5.85	2.48
0.5	5	20.89	21.23	1.58	4.22	4.26	0.93
1	5	18.19	18.46	1.46	2.71	2.66	1.96
0	2	18.78	19.10	1.69	2.92	2.99	2.41
0.5	2	16.91	17.08	1.00	2.03	1.99	2.05
1	2	14.77	14.77	0.01	1.03	1.05	1.52
0	1	14.56	14.58	0.11	1.00	0.98	1.91
0.5	1	12.93	12.89	0.30	0.45	0.45	0.38
1	1	11.14	11.08	0.56	0.00	0.00	0

σ_y = 100, σ_x = 0

* - strict solution obtained by substituting equations (7) to (6); $Error = \left|\dfrac{K_j^{\lambda_r} / a - K_j^{\lambda_r *} / a}{K_j^{\lambda_r *} / a}\right| 100\%$

Table 2

Values of coefficients $K_j^{\lambda_r}/a$ for simultaneous tensile perpendicular and parallel to interface

$\nu_0 = \nu_2 / \nu_1$	$\Gamma_0 = E_2 / E_1$	$K_I^{\lambda_r} / a$	$K_I^{\lambda_r *} / a$	*Error*, %	$K_{II}^{\lambda_r} / a$	$K_{II}^{\lambda_r *} / a$	*Error*, %
0	10	17.42	17.79	2.04	5.11	5.22	2.17
0.5	10	15.70	16.17	2.89	3.79	3.90	2.79
1	10	13.86	14.10	1.73	2.57	2.51	2.37
0	5	16.18	16.43	1.52	3.99	4.10	2.74
0.5	5	14.57	14.86	1.95	2.91	2.98	2.40
1	5	12.78	12.92	1.14	1.85	1.86	0.46
0	2	13.14	13.37	1.74	2.11	2.10	0.78
0.5	2	11.80	11.96	1.35	1.38	1.39	1.01
1	2	10.32	10.34	0.21	0.74	0.73	1.00
0	1	10.14	10.20	0.58	0.67	0.69	1.78
0.5	1	9.04	9.02	0.15	0.32	0.31	1.23
1	1	7.80	7.75	0.58	0.00	0.00	0

σ_y = 100, σ_x =10

* - strict solution obtained by substituting equations (7) to (6); $Error = \left|\dfrac{K_j^{\lambda_r} / a - K_j^{\lambda_r *} / a}{K_j^{\lambda_r *} / a}\right| 100\%$

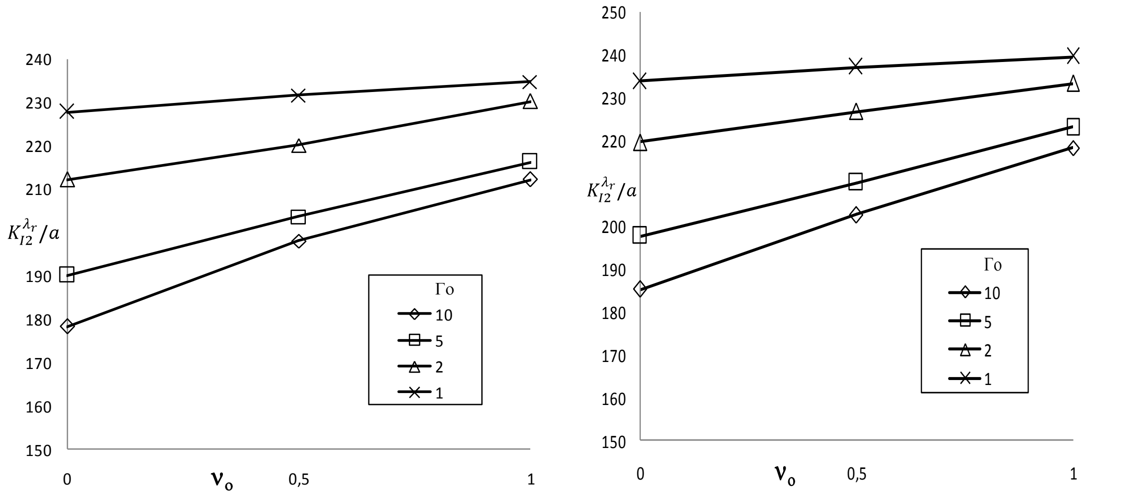

a b

Fig. 5 Constant $K_{I2}^{\lambda_r} / a$ at second term: a - tensile transverse; b - tensile perpendicular and parallel to interface

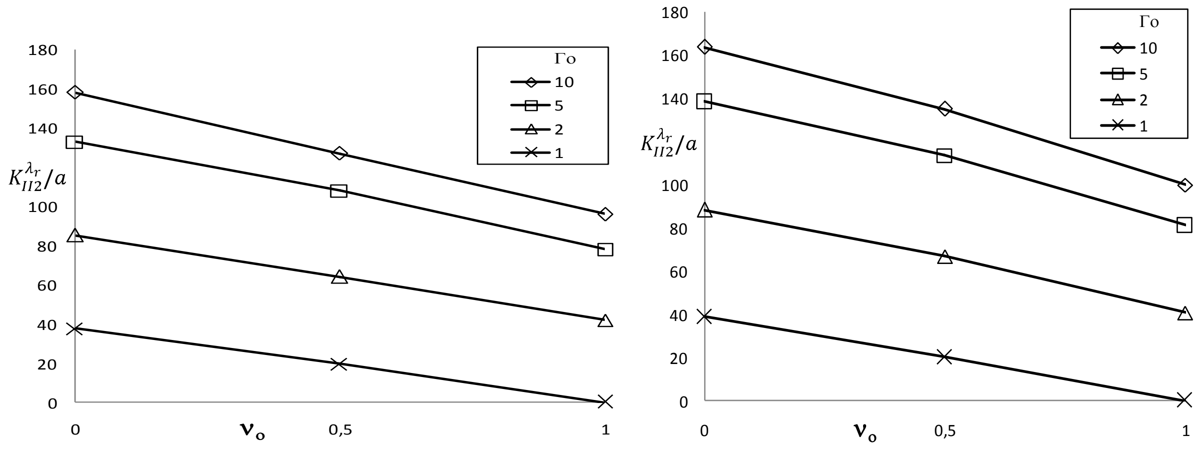

a b

Fig. 6 Constant $K_{II2}^{\lambda_r} / a$ at second term: a - tensile transverse; b - tensile perpendicular and parallel to interface

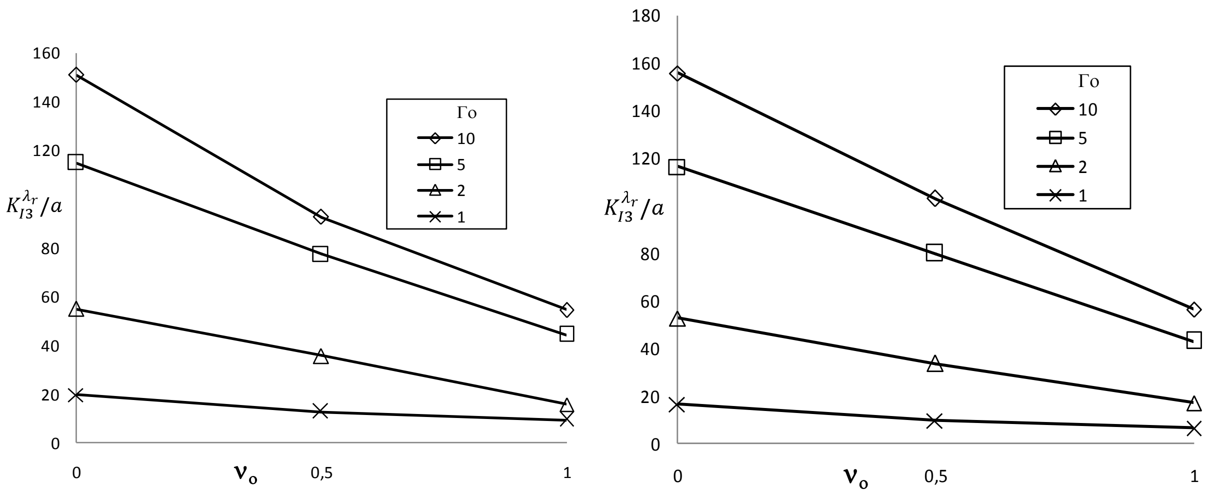

a b

Fig. 7 Constant $K_{I3}^{\lambda_r} / a$ at third term: a - tensile transverse; b - tensile perpendicular and parallel to interface

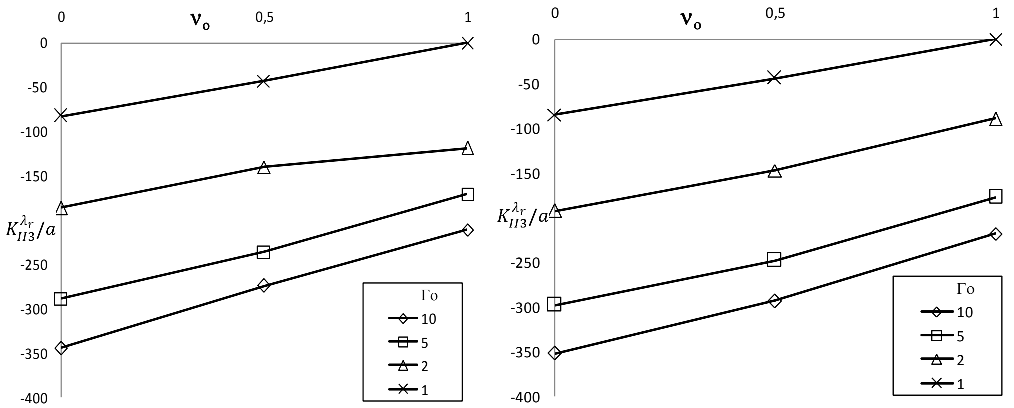

a b

Fig. 8 Constant $K_{II3}^{\lambda_r}$ / a at third term: a - tensile transverse; b - tensile perpendicular and parallel to interface

When analyzing Figs. 5-8, it can be concluded that for both load cases coefficients of higher order terms $K_{I3}^{\lambda_r}, K_{II2}^{\lambda_r}$ increase the diversity of materials, while $K_{I2}^{\lambda_r}, K_{II3}^{\lambda_r}$ decrease.

5. Summary and conclusions

This paper presents the results of investigating a flat element of two-phase structure with sharp linear inclusion located at the interface.

Analytical description of fields of stresses and displacements at the tip of a sharp rigid inclusion was obtained as an asymptotic. It has been presented as a function of the modified stress intensity factors. Relationship between the classically defined stress intensity factors K_I, K_{II} and modified coefficients $K_I^{\lambda_r}$, $K_{II}^{\lambda_r}$ has been defined. Possibility of using different methods (e.g. the FEM) to determine the modified coefficients has also been discussed.

On basis of this study, the following conclusions can be drawn:

- exponent λ takes complex values for the odd terms of the asymptotic expansion and real for even;
- components of stresses and displacements, at the same time, always depend on $K_I^{\lambda_r}$ and $K_{II}^{\lambda_r}$ and for independently acting normal and tangential loads;
- calculated coefficients $K_I^{\lambda_r}$ and $K_{II}^{\lambda_r}$ comply with the exact solution and are subject to error not greater than 3%;
- value ratios $K_I^{\lambda_r}$ and $K_{II}^{\lambda_r}$ are subject to increase along with the diversity of material constants;
- for both the applied load cases, constant values $K_{I3}^{\lambda_r}, K_{II2}^{\lambda_r}$ increase the diversity of materials, while $K_{I2}^{\lambda_r}, K_{II3}^{\lambda_r}$ decrease;
- the method used to determine value of the modified stress intensity factors is not sensitive to material parameters variation;
- use higher order terms increases accuracy of the results.

References

1. **Brahtz, J.H.A.** 1933. Stress distribution in a reentrant corner, Trans. ASME 55: 31-37.
2. **Erdogan, F.** 1963. Stress distribution in a nonhomogeneous elastic plane with cracks, Trans. ASME, Ser. E, J. Applied Mechanics 30: 232-236. http://dx.doi.org/10.1115/1.3636517.
3. **Murakami, Y. ed.** 1987. Stress Intensity Factors Handbook, Pergamon Press. http://www.amazon.com/Stress-Intensity-Factors-Handbook-Murakami/dp/0080348092.
4. **Sih, G.C.; Chen, E.P.** 1981. Cracks in Composite Materials, Ch.3 (Mechanics of Fracture VI) ed. G. C. Sih, Martinus Nijhoff Publishers. http://dx.doi.org/10.1007/978-94-009-8340-3.
5. **Chen, D.H.** 1992. Analysis for corner singularity in composite materials based on the body force method. Computational Methods in Fracture Mechanics, Fatigue and Fracture Mechanics, Comp. Mech. Publ., Southampton), 397-421.
6. **Wang, Z.Y.; Zhang, H.T.; Chou, Y.T.** 1985. Characteristics of the elastic field of a rigid line inhomogeneity, Journal of Applied Mechanics 52: 818-822. http://dx.doi.org/10.1115/1.3169152.
7. **Ballarini, R.** 1987. An integral equation approach for rigid line inhomogeneity problems, International Journal of Fracture 33: 23-26. http://dx.doi.org/10.1007/BF00033747.
8. **Wu, K.C.** 1990. Line inclusions at anisotropic bimaterial interface, Mechanics of Materials 10: 173-182. http://dx.doi.org/10.1016/0167-6636(90)90041-D.
9. **Ballarini, R.** 1990. Rigid line inclusion at a bimaterial interface, Engineering Fracture Mechanics 37: 1-5. http://dx.doi.org/10.1016/0013-7944(90)90326-C.
10. **Asundi, A.** 1995. W. Deng , Rigid inclusions on the interface between dissimilar anisotropic media, Journal of the Mechanics and Physics of Solids 43(7): 1045-1058. http://dx.doi.org/10.1016/0022-5096(95)00022-B.
11. **Spinu, S.** 2013 A refined numerical solution to the inclusion problem, Mechanika 19(3): 252-259. http://dx.doi.org/10.5755/j01.mech.19.3.4657.
12. **Muskhelishvili, N.I.** 1963. Some Basic Problems of the Mathematical Theory of Elasticity, Noordhoff, Leiden.

http://dx.doi.org/10.1007/978-94-017-3034-1.

13. **Dong, C.Y.** 2008. The integral equation formulations of an infinite elastic medium containing inclusions, cracks and rigid lines, Engineering Fracture Mechanics 75: 3952-3965.
http://dx.doi.org/10.1016/j.engfracmech.2008.03.004
14. **Mochalov, E.V.; Sil'vestrov, V.V.** 2011. Problem of interaction of thin rigid needle-shaped inclusion, Mechanics of Solids 46(5): 739-754.
http://dx.doi.org/10.3103/S0025654411050086.
15. **Lee, K.Y.; Kwak, S.G.** 2002. Determination of stress intensity factors for bimaterial interface stationary rigid line inclusions by boundary element method, International Journal of Fracture 113: 285-294.
http://dx.doi.org/10.1023/A:1014281405088.
16. **Lin, K.Y.; Mar, J.W.** 1976. Finite element analysis of stress intensity factors for cracks at a bi-material interface, International Journal of Fracture 12(4): 521-531.
http://dx.doi.org/10.1007/BF00034638
17. **Parton, V.Z.; Perlin, P.I.** 1984. Mathematical Methods of the Theory of Elasticity, Mir Publishers, Moscow.
http://www.amazon.com/Mathematical-Methods-Theory-Elasticity-VOLUMES/dp/0828529329.
18. **Tracey, D.M.** 1971. Finite elements for determination of crack tip elastic stress intensity factors, Engineering Fracture Mechanics 3(3): 255-265.
http://dx.doi.org/10.1016/0013-7944(71)90036-1.
19. **Dundurs, J.** 1967. Effect of elastic constants on stress in a composite under plane deformation, J. Comp. Mater 1: 310-322.
http://dx.doi.org/10.1177/002199836700100306.
20. **Wilson, W.K.** 1973. Finite element methods for elastic bodies containing cracks, Mechanics of Fracture 1: 484-515.
http://dx.doi.org/10.1007/978-94-017-2260-5_9.
21. **Rice, J.R.** 1968. A path independent integral and approximate analysis of strain concentration by notches and cracks, Journal of Applied Mechanics 35(2): 379-386.
http://dx.doi.org/10.1115/1.3601206.
22. **Parks, D.M.** 1974. A stiffness derivative finite element technique for determination of crack tip stress intensity factors, International Journal of Fracture 10(1): 487-502.
http://dx.doi.org/10.1007/BF00155252.
23. **Byskov, E.** 1970. Calculation of stress intensity factors using finite element method with cracked elements, International Journal of Fracture Mechanics 6(2): 159-167.
http://dx.doi.org/10.1007/BF00189823.
24. **Hilton, P.D.G.; Sih, C.** 1973. Applications of the finite element method to the calculations of stress intensity factors, Mechanics of Fracture 1: 426-482.
http://dx.doi.org/10.1007/978-94-017-2260-5_8.
25. **Mieczkowski, G.; Molski, K.; Seweryn, A.** 2007. Finite element modelling of stresses and displacements near the tips of pointed inclusions, Materials Science 42: 183-194.
http://dx.doi.org/10.1007/s11003-007-0021-4.

G. Mieczkowski

DESCRIPTION OF STRESS FIELDS AND DISPLACEMENTS AT THE TIP OF A RIGID, FLAT INCLUSION LOCATED AT INTERFACE USING MODIFIED STRESS INTENSITY FACTORS

S u m m a r y

This paper presents the results of investigating a flat element of two-phase structure with sharp linear inclusion located at the interface. Analytical description of fields of stresses and displacements at the tip of a sharp rigid inclusion was obtained as an asymptotic. It was presented as a function of modified stress intensity factors. Relationship between the classically defined stress intensity factors K_I , K_{II} and modified coefficients $K_I^{\lambda r}$, $K_{II}^{\lambda r}$ has been defined. Possibility of using different methods (e.g. the FEM) set on determining coefficients $K_j^{\lambda r}$ has been discussed, and thus these values have been calculated numerically and compared with the exact solution.

Keywords: fracture, bimaterial; rigid inclusion; singular stress fields; stress intensity factors.

Received November 19, 2014
Accepted March 12, 2015

Appendix
Stresses and displacements fields

$$f_{rr}^{\mathrm{I}} = -5cos\left[\Delta-\frac{\varphi}{2}\right] - cos[\Delta+\frac{3\varphi}{2}] + 4\epsilon\, cos[\Delta+\frac{\varphi}{2}]sin[\varphi] + 2cos[\Delta+\frac{3\varphi}{2}]\kappa_j + \mathrm{e}^{2\epsilon\varphi}(3cos\left[\Delta-\frac{3\varphi}{2}\right] + 5cos\left[\Delta+\frac{\varphi}{2}\right] + 4\epsilon\, cos[\Delta-\frac{\varphi}{2}]sin[\varphi])\kappa_j +$$
$$+\mathrm{e}^{2\pi\epsilon}\left(5cos\left[\Delta-\frac{\varphi}{2}\right] + 3cos[\Delta+\frac{3\varphi}{2}] - 4\epsilon\, cos[\Delta+\frac{\varphi}{2}]sin[\varphi]\right)\kappa_j + \mathrm{e}^{2\epsilon(\pi+\varphi)}\kappa_j\left(cos\left[\Delta-\frac{3\varphi}{2}\right] + 5cos[\Delta+\frac{\varphi}{2}] + 4\epsilon\, cos[\Delta-\frac{\varphi}{2}]sin[\varphi] - 2cos[\Delta-\frac{3\varphi}{2}]\kappa_j\right),$$

$$f_{rr}^{II} = -5sin\left[\Delta-\frac{\varphi}{2}\right] + 4\epsilon\, sin\left[\Delta+\frac{\varphi}{2}\right]sin[\varphi] - sin\left[\Delta+\frac{3\varphi}{2}\right] + \mathrm{e}^{2\epsilon\varphi}\left(3sin\left[\Delta-\frac{3\varphi}{2}\right] + 5sin\left[\Delta+\frac{\varphi}{2}\right] + 4\epsilon\, sin\left[\Delta-\frac{\varphi}{2}\right]sin[\varphi]\right)\kappa_j + 2sin\left[\Delta+\frac{3\varphi}{2}\right]\kappa_j +$$
$$+\mathrm{e}^{2\pi\epsilon}\left(5sin\left[\Delta-\frac{\varphi}{2}\right] - 4\epsilon\, sin\left[\Delta+\frac{\varphi}{2}\right]sin[\varphi] + 3sin\left[\Delta+\frac{3\varphi}{2}\right]\right)\kappa_j + \mathrm{e}^{2\epsilon(\pi+\varphi)}\kappa_j\left(sin\left[\Delta-\frac{3\varphi}{2}\right] + 5sin\left[\Delta+\frac{\varphi}{2}\right] + 4\epsilon\, sin\left[\Delta-\frac{\varphi}{2}\right]sin[\varphi] - 2sin\left[\Delta-\frac{3\varphi}{2}\right]\kappa_j\right),$$

$$f_{\varphi\varphi}^{I} = -3cos\left[\Delta-\frac{\varphi}{2}\right] + cos\left[\Delta+\frac{3\varphi}{2}\right] - 4\epsilon\, cos\left[\Delta+\frac{\varphi}{2}\right]sin[\varphi] - 2cos\left[\Delta+\frac{3\varphi}{2}\right]\kappa_j - 2\mathrm{e}^{2\epsilon\varphi}\left(2\epsilon\, cos\left[\Delta-\frac{\varphi}{2}\right] + 3sin\left[\Delta-\frac{\varphi}{2}\right]\right)sin[\varphi]\kappa_j +$$
$$+2\mathrm{e}^{2\pi\epsilon}\left(2\epsilon\, cos\left[\Delta+\frac{\varphi}{2}\right] + 3sin\left[\Delta+\frac{\varphi}{2}\right]\right)sin[\varphi]\kappa_j + \mathrm{e}^{2\epsilon(\pi+\varphi)}\kappa_j\left(-cos\left[\Delta-\frac{3\varphi}{2}\right] + 3cos\left[\Delta+\frac{\varphi}{2}\right] - 4\epsilon\, cos\left[\Delta-\frac{\varphi}{2}\right]sin[\varphi] + 2cos\left[\Delta-\frac{3\varphi}{2}\right]\kappa_j\right),$$

$$\begin{aligned}
f_{\varphi\varphi}^{II} ={}& -3\,sin\left[\Delta-\frac{\varphi}{2}\right]-4\epsilon\,sin\left[\Delta+\frac{\varphi}{2}\right]sin[\varphi]+sin\left[\Delta+\frac{3\varphi}{2}\right]+2\mathrm{e}^{2\epsilon\varphi}\left(3cos\left[\Delta-\frac{\varphi}{2}\right]-2\epsilon\,sin\left[\Delta-\frac{\varphi}{2}\right]\right)sin[\varphi]\kappa_j+\\
&+2\mathrm{e}^{2\pi\epsilon}\left(-3cos\left[\Delta+\frac{\varphi}{2}\right]+2\epsilon\,sin\left[\Delta+\frac{\varphi}{2}\right]\right)sin[\varphi]\kappa_j-2\,sin\left[\Delta+\frac{3\varphi}{2}\right]\kappa_j+\mathrm{e}^{2\epsilon(\pi+\varphi)}\kappa_j\left(-sin\left[\Delta-\frac{3\varphi}{2}\right]+3sin\left[\Delta+\frac{\varphi}{2}\right]-4\epsilon\,sin\left[\Delta-\frac{\varphi}{2}\right]sin[\varphi]+2\,sin\left[\Delta-\frac{3\varphi}{2}\right]\kappa_j\right),
\end{aligned}$$

$$\begin{aligned}
f_{r\varphi}^{I} ={}& 2\,sin\left[\Delta+\frac{\varphi}{2}\right](cos[\varphi]-2\epsilon\,sin[\varphi])+\mathrm{e}^{2\epsilon\varphi}\left(3sin\left[\Delta-\frac{3\varphi}{2}\right]+sin\left[\Delta+\frac{\varphi}{2}\right]+4\epsilon\,sin\left[\Delta-\frac{\varphi}{2}\right]sin[\varphi]\right)\kappa_j+\\
&+\mathrm{e}^{2\pi\epsilon}\left(-sin\left[\Delta-\frac{\varphi}{2}\right]+4\epsilon\,sin\left[\Delta+\frac{\varphi}{2}\right]sin[\varphi]-3sin\left[\Delta+\frac{3\varphi}{2}\right]\right)\kappa_j-2\,sin\left[\Delta+\frac{3\varphi}{2}\right]\kappa_j+\mathrm{e}^{2\epsilon(\pi+\varphi)}\kappa_j\left(2\,sin\left[\Delta-\frac{\varphi}{2}\right](cos[\varphi]+2\epsilon\,sin[\varphi])-2\,sin\left[\Delta-\frac{3\varphi}{2}\right]\kappa_j\right),
\end{aligned}$$

$$\begin{aligned}
f_{r\varphi}^{II} ={}& -2\,cos\left[\Delta+\frac{\varphi}{2}\right](cos[\varphi]-2\epsilon\,sin[\varphi])+2\,cos\left[\Delta+\frac{3\varphi}{2}\right]\kappa_j+\mathrm{e}^{2\epsilon\varphi}\left(-3cos\left[\Delta-\frac{3\varphi}{2}\right]-cos\left[\Delta+\frac{\varphi}{2}\right]-4\epsilon\,cos\left[\Delta-\frac{\varphi}{2}\right]sin[\varphi]\right)\kappa_j+\\
&+\mathrm{e}^{2\pi\epsilon}\left(cos\left[\Delta-\frac{\varphi}{2}\right]+3cos\left[\Delta+\frac{3\varphi}{2}\right]-4\epsilon\,cos\left[\Delta+\frac{\varphi}{2}\right]sin[\varphi]\right)\kappa_j+2\mathrm{e}^{2\epsilon(\pi+\varphi)}\kappa_j\left(-cos\left[\Delta-\frac{\varphi}{2}\right](cos[\varphi]+2\epsilon\,sin[\varphi])+cos\left[\Delta-\frac{3\varphi}{2}\right]\kappa_j\right),
\end{aligned}$$

$$\begin{aligned}
g_{r}^{I} ={}& 2\,sin[\varphi]\left(\left(1+4\epsilon^2\right)sin\left[\Delta+\frac{\varphi}{2}\right]+\left(4\epsilon\,cos\left[\Delta+\frac{\varphi}{2}\right]-2\,sin\left[\Delta+\frac{\varphi}{2}\right]\right)\kappa_j\right)+\\
&+\mathrm{e}^{2\epsilon\varphi}\kappa_j\left(\left(3+4\epsilon^2\right)cos\left[\Delta-\frac{3\varphi}{2}\right]-\left(1+4\epsilon^2\right)cos\left[\Delta+\frac{\varphi}{2}\right]+4\epsilon\,sin\left[\Delta-\frac{3\varphi}{2}\right]+2\left(cos\left[\Delta+\frac{\varphi}{2}\right]+2\epsilon\,sin\left[\Delta+\frac{\varphi}{2}\right]\right)\kappa_j\right)+\\
&+\mathrm{e}^{2\pi\epsilon}\kappa_j\begin{pmatrix}\left(-1-4\epsilon^2\right)cos\left[\Delta-\frac{\varphi}{2}\right]+\left(3+4\epsilon^2\right)cos\left[\Delta+\frac{3\varphi}{2}\right]+\\
+2\mathrm{e}^{2\epsilon\varphi}\left(1+4\epsilon^2\right)sin\left[\Delta-\frac{\varphi}{2}\right]sin[\varphi]+4\epsilon\,sin\left[\Delta+\frac{3\varphi}{2}\right]+2\left(2\,sin\left[\Delta-\frac{\varphi}{2}\right]\left(\epsilon-\mathrm{e}^{2\epsilon\varphi}\,sin[\varphi]\right)+cos\left[\Delta-\frac{\varphi}{2}\right]\left(1+4\mathrm{e}^{2\epsilon\varphi}\epsilon\,sin[\varphi]\right)\right)\kappa_j\end{pmatrix},
\end{aligned}$$

$$\begin{aligned}
g_{r}^{II} ={}& -2\,cos\left[\Delta+\frac{\varphi}{2}\right]sin[\varphi]-8\epsilon^2\,cos\left[\Delta+\frac{\varphi}{2}\right]sin[\varphi]+4\,cos\left[\Delta+\frac{\varphi}{2}\right]sin[\varphi]\kappa_j+8\epsilon\,sin\left[\Delta+\frac{\varphi}{2}\right]sin[\varphi]\kappa_j-\\
&-\mathrm{e}^{2\epsilon\varphi}\kappa_j\left(-3\,sin\left[\Delta-\frac{3\varphi}{2}\right]+sin\left[\Delta+\frac{\varphi}{2}\right]+4\epsilon\left(cos\left[\Delta-\frac{3\varphi}{2}\right]+2\epsilon\,cos\left[\Delta-\frac{\varphi}{2}\right]sin[\varphi]\right)-2\begin{pmatrix}-2\epsilon\,cos\left[\Delta+\frac{\varphi}{2}\right]+\\
+\mathrm{e}^{2\pi\epsilon}\left(2\epsilon\,cos\left[\Delta-\frac{3\varphi}{2}\right]-sin\left[\Delta-\frac{3\varphi}{2}\right]\right)+sin\left[\Delta+\frac{\varphi}{2}\right]\end{pmatrix}\kappa_j\right)+\\
&+\mathrm{e}^{2\pi\epsilon}\kappa_j\begin{pmatrix}-4\epsilon\,cos\left[\Delta+\frac{3\varphi}{2}\right]-sin\left[\Delta-\frac{\varphi}{2}\right]-2\mathrm{e}^{2\epsilon\varphi}\left(1+4\epsilon^2\right)cos\left[\Delta-\frac{\varphi}{2}\right]sin[\varphi]+8\epsilon^2\,cos\left[\Delta+\frac{\varphi}{2}\right]sin[\varphi]+3\,sin\left[\Delta+\frac{3\varphi}{2}\right]+\\
+2\left(\left(-1-\mathrm{e}^{2\epsilon\varphi}\right)cos\left[\frac{\varphi}{2}\right](2\epsilon\,cos[\Delta]-sin[\Delta])+\left(-1+\mathrm{e}^{2\epsilon\varphi}\right)(cos[\Delta]+2\epsilon\,sin[\Delta])sin\left[\frac{\varphi}{2}\right]\right)\kappa_j\end{pmatrix},
\end{aligned}$$

$$\begin{aligned}
g_{\varphi}^{I} ={}& -\mathrm{e}^{2\epsilon(\pi+\varphi)}\,sin\left[\Delta-\frac{3\varphi}{2}\right]\kappa_j-2\mathrm{e}^{2\pi\epsilon}\,cos\left[\Delta+\frac{\varphi}{2}\right]\kappa_j\left(sin[\varphi]+4\epsilon^2\,sin[\varphi]+4\epsilon\,cos[\varphi]\kappa_j\right)\times\\
&\times\left(-4\epsilon\,cos\left[\Delta+\frac{3\varphi}{2}\right]-\left(1+4\epsilon^2\right)sin\left[\Delta-\frac{\varphi}{2}\right]+\left(3+4\epsilon^2\right)sin\left[\Delta+\frac{3\varphi}{2}\right]+\left(4\epsilon\,cos\left[\Delta-\frac{\varphi}{2}\right]-2\,sin\left[\Delta-\frac{\varphi}{2}\right]\right)\kappa_j\right)+\\
&+\mathrm{e}^{2\epsilon\varphi}\kappa_j\left(4\epsilon\,cos\left[\Delta-\frac{3\varphi}{2}\right]-\left(3+4\epsilon^2\right)sin\left[\Delta-\frac{3\varphi}{2}\right]+\left(1+4\epsilon^2\right)sin\left[\Delta+\frac{\varphi}{2}\right]+2\left(-2\epsilon\,cos\left[\Delta+\frac{\varphi}{2}\right]+sin\left[\Delta+\frac{\varphi}{2}\right]\right)\kappa_j\right)-\\
&-\kappa_j\left(4cos[\varphi]sin\left[\Delta+\frac{\varphi}{2}\right]+\mathrm{e}^{2\epsilon(\pi+\varphi)}\left(8\epsilon^2\,cos[\varphi]sin\left[\Delta-\frac{\varphi}{2}\right]+sin\left[\Delta+\frac{\varphi}{2}\right]+4\,cos[\varphi]\left(-2\epsilon\,cos\left[\Delta-\frac{\varphi}{2}\right]+sin\left[\Delta-\frac{\varphi}{2}\right]\right)\kappa_j\right)\right),
\end{aligned}$$

$$\begin{aligned}
g_{\varphi}^{II} ={}& 2\left(1+4\epsilon^2\right)sin\left[\Delta+\frac{\varphi}{2}\right]sin[\varphi]+\left(cos\left[\Delta+\frac{\varphi}{2}\right]\left(\mathrm{e}^{2\epsilon(\pi+\varphi)}\left(1+4\epsilon^2\right)+4\,cos[\varphi]\right)+8\epsilon\,cos[\varphi]sin\left[\Delta+\frac{\varphi}{2}\right]\right)\kappa_j+\\
&+4\mathrm{e}^{2\epsilon(\pi+\varphi)}\,cos[\varphi]\left(cos\left[\Delta-\frac{\varphi}{2}\right]+2\epsilon\,sin\left[\Delta-\frac{\varphi}{2}\right]\right)\kappa_j^2-\\
&-\mathrm{e}^{2\pi\epsilon}\kappa_j\left(\mathrm{e}^{2\epsilon\varphi}\left(1+4\epsilon^2\right)cos\left[\Delta-\frac{3\varphi}{2}\right]+cos\left[\Delta-\frac{\varphi}{2}\right]-3cos\left[\Delta+\frac{3\varphi}{2}\right]+8\epsilon^2\,sin\left[\Delta+\frac{\varphi}{2}\right]sin[\varphi]-4\epsilon\,sin\left[\Delta+\frac{3\varphi}{2}\right]+2\left(cos\left[\Delta-\frac{\varphi}{2}\right]+2\epsilon\,sin\left[\Delta-\frac{\varphi}{2}\right]\right)\kappa_j\right)+\\
&+\mathrm{e}^{2\epsilon\varphi}\kappa_j\left(\left(-3-4\epsilon^2\right)cos\left[\Delta-\frac{3\varphi}{2}\right]+\left(1+4\epsilon^2\right)cos\left[\Delta+\frac{\varphi}{2}\right]-4\epsilon\,sin\left[\Delta-\frac{3\varphi}{2}\right]+2\left(cos\left[\Delta+\frac{\varphi}{2}\right]+2\epsilon\,sin\left[\Delta+\frac{\varphi}{2}\right]\right)\kappa_j\right),
\end{aligned}$$

where $\Delta=\epsilon\,log[r]$.